Enhancement of tunnel magnetoresistance in magnetic tunnel junction by a superlattice barrier

C. H. Chen and W. J. Hsueh

Citation: Applied Physics Letters **104**, 042405 (2014); doi: 10.1063/1.4863221
View online: http://dx.doi.org/10.1063/1.4863221
View Table of Contents: http://scitation.aip.org/content/aip/journal/apl/104/4?ver=pdfcov
Published by the AIP Publishing

Enhancement of tunnel magnetoresistance in magnetic tunnel junction by a superlattice barrier

C. H. Chen and W. J. Hsueh[a)]
Nanomagnetism Group, Department of Engineering Science and Ocean Engineering, National Taiwan University, 1, Sec. 4, Roosevelt Road, Taipei 10660, Taiwan

(Received 12 November 2013; accepted 11 January 2014; published online 30 January 2014)

Tunnel magnetoresistance of magnetic tunnel junction improved by a superlattice barrier composed of alternate layers of a nonmagnetic metal and an insulator is proposed. The forbidden band of the superlattice is used to predict the low transmission range in the superlattice barrier. By forbidding electron transport in the anti-parallel configuration, the tunnel magnetoresistance is enhanced in the superlattice junction. The results show that the tunnel magnetoresistance ratio for a superlattice magnetic tunnel junction is greater than that for traditional single or double barrier junctions. © *2014 AIP Publishing LLC*. [http://dx.doi.org/10.1063/1.4863221]

An emerging field of electronics, called spintronics, has been developing rapidly for systems such as magnetic semiconductors, metallic magnetic multilayers, and strongly correlated electron systems.[1,2] Of these systems, magnetic tunnel junctions (MTJ) have attracted widespread attention because of their potential applications in nonvolatile magnetic random access memories, weak magnetic field sensors, and other spintronics devices.[3–5] A giant tunnel magnetoresistance (TMR) at room temperature was first found in a ferromagnet/insulator/ferromagnet (F/I/F) magnetic tunnel junction.[6] As well as a single barrier MTJ (SBMTJ), both experimental and theoretical studies of F/I/F/I/F double barrier MTJs (DBMTJ) have also been undertaken.[7]

The concept of a superlattice, which is a man-made material that consists of alternating layers of two dissimilar materials with layer thicknesses of the order of nanometers, has been used in fields such as photonics,[8–11] spintronics,[12–14] and electronics.[15,16] One of the most important advantages of a superlattice is its flexibility, compared to a natural material. The band structure of a superlattice is specified by adjusting the parameters of the superlattice. A semiconductor superlattice, which has many interesting properties, such as a miniband structure and negative differential conductivity, is composed of two different semiconductors, such as GaAs and AlAs. Important optoelectronic devices, such as infrared photodetectors and high electron mobility transistors, have been produced using a semiconductor superlattice.[15,16] However, magnetic superlattices, which are composed of two different magnetic materials, have special properties, such as their giant magnetoresistance effect and their magnonic bandgap. These properties are useful in the transmission, storage, and processing of information.[12,13]

The theoretical model proposed by Niu *et al*. was used to interpret the experimental data for DBMTJs in a sequential regime.[17] They found that the TMR ratio for F/I/F/I/F junctions in the sequential regime cannot exceed the larger of the TMR ratios of the two single F/I/F junctions that form the double junction. However, recent studies[18–20] have shown that the TMR ratio for F/I/F/I/F junctions in a coherent tunneling regime can be larger than the corresponding SBMTJs. The TMR ratio has been found to oscillate with variations in the thickness of the middle F layer and can reach large values if this thickness is appropriate.[18] However, both experimental and theoretical studies have shown that inserting nonmagnetic metals into a MTJ is one of the simplest ways to ensure coherent tunneling.[21,22] Although coherent tunneling and the TMR effect for both SBMTJs and DBMTJs that use nonmagnetic metals have been studied,[18,21–23] there have been no studies of a superlattice barrier (SLB) MTJ that uses nonmagnetic metals. It may be possible to take advantage of the superlattice to improve the TMR ratio of a MTJ. In this paper, the TMR of a magnetic tunnel junction is improved, using a superlattice barrier that is composed of alternate layers of a nonmagnetic metal and an insulator. It is found that the formation of the forbidden bands in the SLB can be used to improve the TMR ratio of a MTJ. The tunnel magnetoresistance is more than 10^5% in a SLBMTJ, because electron transport is forbidden in the anti-parallel configuration. The results show that the TMR ratio for a SLBMTJ can be greater than that for a traditional DBMTJ.

Initially, a SLBMTJ with alternating binary nanothickness layers, a nonmagnetic metal layer (N) and an insulating tunnel barrier (I), with both sides enclosed by the same ferromagnetic electrodes is considered. This SLBMTJ is denoted as F_L/SLB/F_R, where $F_{L(R)}$ stands for the ferromagnetic electrode on the left (right) side. The layers in the SLB are perpendicular to the x-axis. A small bias is applied between the two ferromagnetic electrodes. The parabolic band model, originally proposed by Slonczewski,[24] is used to calculate the transmission of spin-up and spin-down electrons. The wave vector parallel to the plane ($k_{||}$) is assumed to be conserved (coherent tunneling). The Schrödinger equation for the wave function for spin-up ($\psi_\uparrow$) and spin down ($\psi_\downarrow$) electrons with an electron mass, m, can be written as

$$\left(-\frac{\hbar^2}{2m}\nabla^2 + U - \vec{h}\cdot\vec{\sigma}\right)\begin{pmatrix}\psi_\uparrow\\ \psi_\downarrow\end{pmatrix} = E\begin{pmatrix}\psi_\uparrow\\ \psi_\downarrow\end{pmatrix}, \quad (1)$$

where $\vec{h}$ is the molecular field[24] and $\vec{\sigma}$ is the Pauli spin operator. U is the potential barrier height. It is assumed that the

[a)]Author to whom correspondence should be addressed. Electronic mail: hsuehwj@ntu.edu.tw. Tel.: 886-2-3366-5750. FAX: 886-2-2392-9885.

fixed magnetization direction of the left-hand side electrode is the same as that of the quantization axis. The magnetization directions in the right-hand side electrodes that are parallel or anti-parallel to the ones in the left-hand side electrodes are termed the parallel configuration and the anti-parallel configuration, respectively. Although $k_{||}$ is neglected in these notations, the effects of summation over $k_{||}$ are considered in the calculations. The wave functions in layer j can be written as $\psi_j^\sigma(x) = A_j^\sigma e^{ik_{x,j}^\sigma(x-x_j)} + B_j^\sigma e^{-ik_{x,j}^\sigma(x-x_j)}$, where A_j^σ and B_j^σ are the amplitudes of the waves in the $+x$ and $-x$ directions, respectively. The superscript, $\sigma = \pm 1$ (or $\sigma = \uparrow, \downarrow$), denotes spin-up and spin-down electrons, respectively. The relationship between the wave functions and their derivatives in both interfaces of the layer can be expressed as

$$\begin{Bmatrix} \psi_j^\sigma \\ \psi_{j-1}^{\sigma'} / m_{j-1} \end{Bmatrix} = \begin{bmatrix} f_j^\sigma & h_j^\sigma \\ g_j^\sigma & f_j^\sigma \end{bmatrix} \begin{Bmatrix} \psi_{j-1}^\sigma \\ \psi_j^{\sigma'} / m_j \end{Bmatrix}, \tag{2}$$

where f_j^σ, g_j^σ, and h_j^σ are $\sec(k_{x,j}^\sigma d_j)$, $(k_{x,j}^\sigma/m_j)\tan(k_{x,j}^\sigma d_j)$, and $(m_j/k_{x,j}^\sigma)\tan(k_{x,j}^\sigma d_j)$, respectively. The wave vector in the x direction can be written as $k_{x,j}^\sigma = [(2m_j/\hbar^2)(E_x - U_j + \sigma\Delta)]^{1/2}$, where Δ is the magnitude of the molecular field and E_x is the transverse components of the total electron energy given by $E_x = E - \hbar^2 k_{||}^2/2m_0$. Thus, E_x is measured from the middle point between the bottoms of the two spin subbands in the left electrode. According to Eq. (2), the relationship between ψ_j^σ, ψ_{j-1}^σ, $(\psi_j^{\sigma'}/m_j)$, and $(\psi_{j-1}^{\sigma'}/m_{j-1})$ can be represented as a two-way graph model.[25] At the boundary of each layer, the wave function, ψ^σ, and its derivative $m^{-1}(\partial\psi^\sigma/\partial x)$, must be continuous. Based on the boundary conditions and the graph model, the amplitude and derivative of the wave functions for the entire system can be represented by a lead type model, which connects the graph models for all of the layers of the system. Using topology, the relationship between the amplitude and the derivative of the wave functions at the ends of the system can be expressed as

$$\psi_N^\sigma = f^\sigma \psi_0^\sigma + h^\sigma \left(\psi_N^{\sigma'}/m_N\right), \tag{3a}$$

$$\left(\psi_0^{\sigma'}/m_0\right) = g^\sigma \psi_0^\sigma + f^\sigma \left(\psi_N^{\sigma'}/m_N\right), \tag{3b}$$

where f^σ, g^σ, and h^σ can be calculated using the graph model.[25]

In order to analyze the transmission in $F_L/SLB/F_R$, it is assumed that a wave is incident from the left hand side of the system to the right side. The transmission amplitude of the waves in the system, $t^\sigma = A_{F_R}^\sigma / A_{F_L}^\sigma$, can be expressed as $t^\sigma = 2f^\sigma/[1 - ih^\sigma k_{x,F_R}^\sigma + (ig^\sigma/k_{x,F_L}^\sigma) + (k_{x,F_R}^\sigma/k_{x,F_L}^\sigma)(g^\sigma h^\sigma - f^{\sigma 2})]$. The transmission coefficient of the wave functions that pass through the system is given by $T^\sigma = |t^\sigma|^2$. The tunnel current[26] in the zero-temperature limit is

$$J^\sigma = \frac{2\pi \times m \times e}{h^3} \left[\int_0^{E_F - eV} \int_{E_F - eV - E_x}^{E_F - E_x} T^\sigma dE_{||} dE_x + \int_{E_F - eV}^{E_F} \int_0^{E_F - E_x} T^\sigma dE_{||} dE_x \right]. \tag{4}$$

The total current density is the sum of the current contributed by the spin-up and the spin-down electrons: $J = J^\uparrow + J^\downarrow$. The TMR is defined as $TMR = (J_P - J_{AP})/J_{AP}$, where J_P and J_{AP} are the current densities for the parallel and the anti-parallel configurations, respectively.

Determining the relationship between the band structure of a SLB and the spin-polarized resonant tunneling in the SLB is a major objective of this study. The band structure of a system is calculated using the periodic boundary. According to Floquet's theorem, wave functions in a system with a periodic boundary must obey the Bloch waves $(\psi_N^{\sigma'}/m_N) = (\psi_0^{\sigma'}/m_0)\exp(iK^\sigma L)$ and $\psi_N^\sigma = \psi_0^\sigma \exp(iK^\sigma L)$, where L is the width of the system. The dispersion relation is written as

$$\cos(K^\sigma L) = \frac{1 - g^\sigma h^\sigma + (f^\sigma)^2}{2f^\sigma}. \tag{5}$$

As the Bloch wave number K^σ is complex, the Bloch wave is evanescent when it propagates in the system. Therefore, the forbidden gap is given by condition, $|\cos(K^\sigma L)| > 1$. However, when K^σ is a real value, the Bloch wave is allowed to propagate in the system. The allowed band occurs if $|\cos(K^\sigma L)| \le 1$. Therefore, the kernels of the band structure are the upper and lower bandedges that correspond to $\cos(K^\sigma L) = 1$ and -1, respectively. According to Eq. (5), the upper or lower bandedges are determined using the roots of the upper or lower bandedge functions, Q_{+1}^σ and Q_{-1}^σ, respectively, defined by $Q_u^\sigma = 1 + (f^\sigma)^2 - g^\sigma h^\sigma - 2u^\sigma f^\sigma$, where $u = 1, -1$. Therefore, the band structure can be drawn by using the upper and lower bandedge equations, $Q_{+1}^\sigma = 0$ and $Q_{-1}^\sigma = 0$. According to the bandedge equations, it is not necessary to calculate $\cos(K^\sigma L)$ to determine the allowed or forbidden bands of the band structure.

For the TMR effect in a SLBMTJ and a DBMTJ, as shown in Fig. 1, it is assumed that the left and right electrodes are made of the same ferromagnetic material. The structure of the SLB is [nonmagnetic metal/insulator]^N, where N is equal to three in the calculation. The parameters used in these calculations are the Fermi energy, $E_F = 2.62$ eV, the magnitude of the molecular field in the ferromagnetic electrode, $\Delta = 1.96$ eV, the height of the insulating barrier, $U_I = 3.37$ eV, and the barrier thickness, $d_I = 0.5$ nm.[23,27,28] A bias voltage of $V = 20$ mV is applied to the structure. We also restrict our considerations to the zero temperature limit. The thickness of the

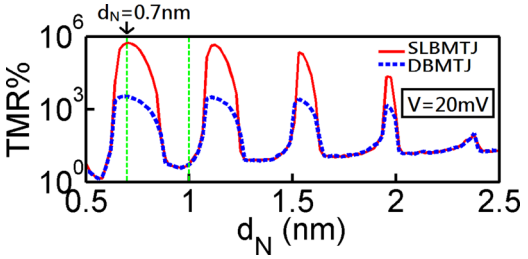

FIG. 1. The TMR as a function of the thickness of the nonmagnetic metal in a SLBMTJ (solid red line) and a DBMTJ (blue dashed line). The parameters are $E_F = 2.62$ eV, $\Delta = 1.96$ eV, $U_I = 3.37$ eV, and $d_I = 0.5$ nm. The corresponding transmission spectra for $d_N = 0.7$ nm is shown in Figs. 2 and 3, for the parallel and the anti-parallel configuration, respectively. The corresponding transmission spectra for anti-parallel configuration with $d_N = 1$nm is shown in Fig. 4.

non-magnetic metal layer is adjusted to observe its effect on the TMR, when the bias voltage, $V = 20\,\text{mV}$, is applied to the junction. The plot of the TMR as a function of d_N has several peaks, the height of which decrease as d_N increases. For the SLBMTJ, the first peak, which corresponds to $TMR \approx 5 \times 10^5\%$ is at $d_N = 0.7\,\text{nm}$. It is to be expected that the periodic oscillation of the TMR as d_N increases is related to the quantum-well states that are formed in the non-magnetic metals and to the resonant tunneling mechanism throughout the entire system.[18,22] The TMR ratio for the double-barrier junction is also shown in Fig. 1. It is seen that the TMR ratio for a SLBMTJ is greater than that for a DBMTJ.

In order to determine why a maximum TMR occurs at certain thicknesses and why the TMR for a SLBMTJ is larger than that for a DBMTJ the transmission spectra of the spin-up and the spin-down electrons are analyzed.[18] The transmission spectra are calculated for the parallel and the anti-parallel configurations, for $d_N = 0.7\,\text{nm}$. The transmission spectra and dispersion relations for the parallel configuration are first considered, as shown in Fig. 2. For a SLBMTJ, the spin-up electrons on the left electrode tunnel through the SLB into the electrode on the right side. These resonance peaks occur in the energy range of the corresponding allowed band that is formed by a SLB. Within the energy range of each corresponding allowed band, there are two resonance peaks. This is because there are two quantum wells in a 3-cell SLB. Therefore, the number of resonant peaks in the energy range of the corresponding allowed band for an n-cell SLB is equal to n-1. However, the transmission probability for spin-down electrons is low since the energy range (Δ, E_F) corresponds to a forbidden band of the SLB. In order to compare the difference in electron transport in a DBMTJ and a SLBMTJ, the transmission spectra for the DBMTJ are also shown in Fig. 2(b). It is seen that there are only two resonance peaks for the spin up electron and none for the spin down electron. In contrast to a SLBMTJ, the probability of transmission does not decrease to an extremely small value when resonant tunneling does not occur. For both the SLBMTJ and the DBMTJ in a parallel configuration, electrons tunnel through the barrier by resonant tunnelling.

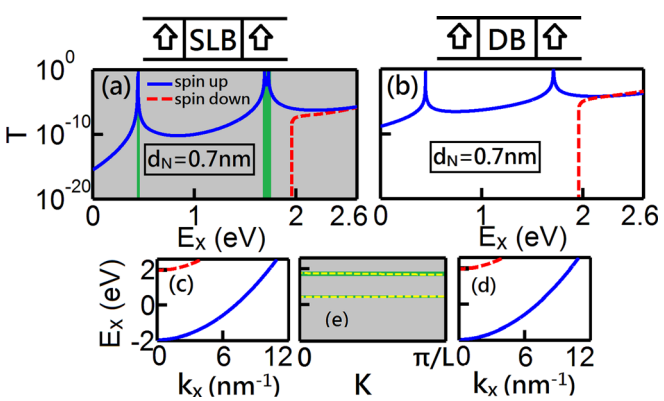

FIG. 2. The transmission spectra for the spin-up (blue solid line) and the spin-down (red dashed line) electrons in (a) a SLBMTJ and (b) a DBMTJ with parallel magnetization of the two electrodes. The dispersion relations of the ferromagnetic electrode on the (c) left and (d) right side, and (e) the SLB. The gray and green areas indicate the forbidden bands and allowed bands of the SLB, respectively. The parameters are the same as those used in Fig. 1, except that $d_N = 0.7\,\text{nm}$.

The transmission spectra and dispersion relations in the anti-parallel configuration are then studied, as shown in Fig. 3. For a SLBMTJ, only the electrons within the energy range (Δ, E_F) can tunnel through the SLB. Below the energy, Δ, there is no corresponding state for the two electrodes. However, the energy range (Δ, E_F) is fully occupied by the forbidden band that is formed by the SLB, such that both the spin-up and the spin-down electrons are forbidden to transport within this energy range. This is similar to the concept of a complete gap in a photonic crystal, in which the TE mode and the TM mode are forbidden.[8] Similarly to a SLBMTJ, only the electrons within the energy range (Δ, E_F) can tunnel through the barriers in a DBMTJ. However, since there is no concept of a forbidden band for a DBMTJ, the probability of transmission for electrons in a DBMTJ is larger than that in a SLBMTJ, within the energy range (Δ, E_F).

This discussion explains why the TMR ratio for a SLBMTJ can be larger than that for a DBMTJ. By the definition of a TMR ratio, $\text{TMR} = (J_P - J_{AP})/J_{AP}$, it is intuitive that the TMR ratio can be improved by reducing the current density in the antiparallel configuration. As is seen from Eq. (4), the current density is proportional to the integral of the transmission spectra with respect to the energy. Therefore, the current density is reduced by ensuring that the integral of transmission spectra with respect to energy is as small as possible. This is achieved by the forbidden band that is formed by the SLB, where there is low transmission. However, there is no concept of a forbidden band in a DBMTJ, so the transmission cannot be less than that in a SLBMTJ. Therefore, the TMR ratio for a SLBMTJ can be larger than that for a DBMTJ, since the J_{AP} in the former can be smaller than that in the latter.

In order to explain why the TMR ratio is small for some specific thicknesses of the nonmagnetic metal, the transmission spectra and dispersion relations are calculated at $d_N = 1\,\text{nm}$, for the anti-parallel configuration, as shown in Fig. 4. For the SLBMTJ, the forbidden band that is formed by the SLB is indicated by the gray area. Although there are three allowed bands, only the electrons in the allowed band within the energy range (Δ, E_F) are permitted to transport, since the configuration is antiparallel.[23] In contrast to Fig. 3(a), in which

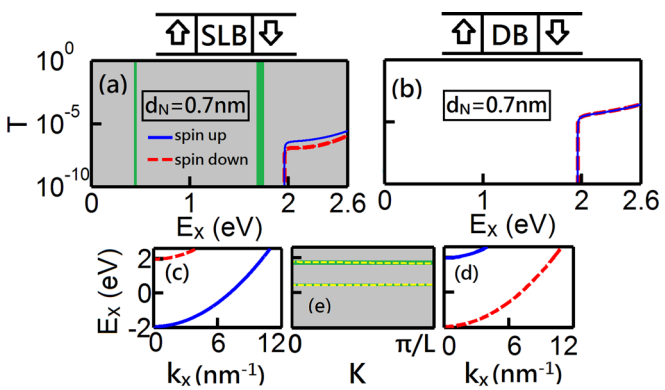

FIG. 3. The transmission spectra for the spin-up (blue solid line) and the spin-down (red dashed line) electrons in (a) a SLBMTJ and (b) a DBMTJ with anti-parallel magnetization of the two electrodes. The dispersion relations of the ferromagnetic electrode on the (c) left and (d) right side, and (e) the SLB. The parameters are the same as those used in Fig. 1, except that $d_N = 0.7\,\text{nm}$.

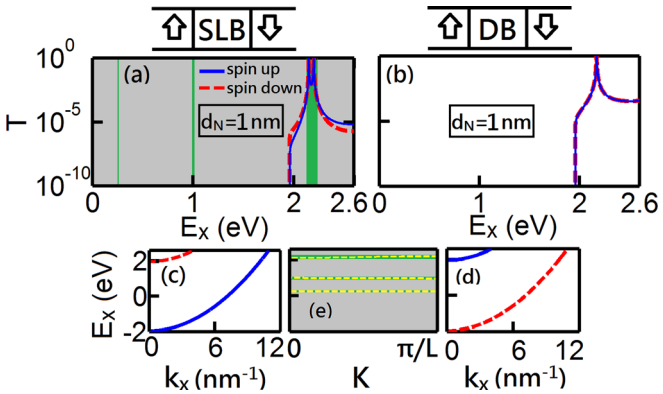

FIG. 4. The transmission spectra for the spin-up (blue solid line) and the spin-down (red dashed line) electrons in (a) a SLBMTJ and (b) a DBMTJ with anti-parallel magnetization of the two electrodes. The dispersion relations of the ferromagnetic electrode on the (c) left and (d) right side, and (e) the SLB. The parameters are the same as those used in Fig. 1, except that $d_N = 1$ nm.

no allowed band exists in the energy range (Δ, E_F), there is an allowed band in the energy range (Δ, E_F) as shown in Fig. 4(a). In the former case, the integral of the transmission spectrum with respect to energy is small, so the TMR ratio is improved. In the latter case, the integral of the transmission spectrum with respect to energy is large, so the TMR ratio is reduced. Therefore, a proper thickness of the layers in the SLB ensures that the energy region (Δ, E_F) can be fully occupied by the forbidden band that is formed by the SLB. This phenomenon causes poor transport of electrons in the antiparallel configuration and thus a huge TMR ratio. On the other hand, there is a resonance peak for the DBMTJ in the antiparallel configuration, as shown in Fig. 4(b). Electrons can be transported through this resonance peak, which results in a large J_{AP} and a small TMR ratio.

In conclusion, the tunnel magnetoresistance effect in a magnetic tunnel junction with a SLB is studied. Compared to a traditional DBMTJ, a greater TMR is possible in a SLBMTJ since the electron transport in the anti-parallel configuration is forbidden. The forbidden band of the SLB is used to predict the low transmission range in the SLB. The TMR oscillates as a function of the thickness of the nonmagnetic metal, which is related to the quantum-well states that are formed in the non-magnetic metals and to the resonant tunneling mechanism throughout the entire system.

The authors acknowledge the support provided by the National Science Council of Taiwan under Grant Nos. NSC 101-2221-E-002-030 and NSC 102-3113-P-002-025.

[1]I. Žutić, J. Fabian, and S. Das Sarma, Rev. Mod. Phys. **76**, 323 (2004).
[2]P. Němec, V. Novák, N. Tesařová, E. Rozkotová, H. Reichlová, D. Butkovičová, F. Trojánek, K. Olejník, P. Malý, R. P. Campion, B. L. Gallagher, J. Sinova, and T. Jungwirth, Nat. Commun. **4**, 1422 (2013).
[3]C. Chappert, A. Fert, and F. N. V. Dau, Nature Mater. **6**, 813 (2007).
[4]Z. M. Zeng, P. K. Amiri, G. Rowlands, H. Zhao, I. N. Krivorotov, J. P. Wang, J. A. Katine, J. Langer, K. Galatsis, K. L. Wang, and H. W. Jiang, Appl. Phys. Lett. **98**, 072512 (2011).
[5]A. Useinov, Y. Saeed, N. Singh, N. Useinov, and U. Schwingenschlögl, Phys. Rev. B **88**, 060405 (2013).
[6]J. S. Moodera, L. R. Kinder, T. M. Wong, and R. Meservey, Phys. Rev. Lett. **74**, 3273 (1995).
[7]J. Barnaś and A. Fert, Phys. Rev. Lett. **80**, 1058 (1998).
[8]W. J. Hsueh, C. T. Chen, and C. H. Chen, Phys. Rev. A **78**, 013836 (2008).
[9]Y. Fink, J. N. Winn, S. Fan, C. Chen, J. Michel, J. D. Joannopoulos, and E. L. Thomas, Science **282**, 1679 (1998).
[10]Q. Xie and C. Lee, Phys. Rev. A **85**, 063802 (2012).
[11]W. J. Hsueh and S. J. Wun, Opt. Lett. **36**, 1581 (2011).
[12]M. N. Baibich, J. M. Broto, A. Fert, F. N. Van Dau, F. Petroff, P. Etienne, G. Creuzet, A. Friederich, and J. Chazelas, Phys. Rev. Lett. **61**, 2472 (1988).
[13]S. V. Grishin, E. N. Beginin, Y. P. Sharaevskii, and S. A. Nikitov, Appl. Phys. Lett. **103**, 022408 (2013).
[14]B. Lenk, H. Ulrichs, F. Garbs, and M. Münzenberg, Phys. Rep. **507**, 107 (2011).
[15]D. Z.-Y. Ting, A. Soibel, A. Khoshakhlagh, J. Nguyen, L. Höglund, S. A. Keo, J. M. Mumolo, and S. D. Gunapala, Appl. Phys. Lett. **102**, 121109 (2013).
[16]G. Ye, H. Wang, S. Arulkumaran, G. I. Ng, R. Hofstetter, Y. Li, M. J. Anand, K. S. Ang, Y. K. T. Maung, and S. C. Foo, Appl. Phys. Lett. **103**, 142109 (2013).
[17]Z. P. Niu, Z. B. Feng, J. Yang, and D. Y. Xing, Phys. Rev. B **73**, 014432 (2006).
[18]A. N. Useinov, J. Kosel, N. K. Useinov, and L. R. Tagirov, Phys. Rev. B **84**, 085424 (2011).
[19]X. Zhang, B. Z. Li, G. Sun, and F. C. Pu, Phys. Rev. B **56**, 5484 (1997).
[20]L. Sheng, Y. Chen, H. Y. Teng, and C. S. Ting, Phys. Rev. B **59**, 480 (1999).
[21]S. Yuasa, T. Nagahama, and Y. Suzuki, Science **297**, 234 (2002).
[22]C. Choi and B. C. Lee, Phys. Rev. B **86**, 134411 (2012).
[23]M. Wilczynski and J. Barnas, J. Magn. Magn. Mater. **221**, 373 (2000).
[24]J. C. Slonczewski, Phys. Rev. B **39**, 6995 (1989).
[25]W. J. Hsueh and H. C. Chen, Phys. Rev. E **76**, 057701 (2007).
[26]F. Montaigne, M. Hehn, and A. Schuhl, Phys. Rev. B **64**, 144402 (2001).
[27]N. N. Beletskii, G. P. Berman, A. R. Bishop, S. A. Borysenko, and V. M. Yakovenko, Phys. Rev. B **75**, 174418 (2007).
[28]C. de Buttet, M. Hehn, F. Montaigne, C. Tiusan, G. Malinowski, A. Schuhl, E. Snoeck, and S. Zoll, Phys. Rev. B **73**, 104439 (2006).